

# Ammonia sensing properties of different polyaniline-based composite nanofibres

Zengyuan Pang, Qingxin Nie, Jie Yang, Fenglin Huang, Yang Xu & Qufu Wei<sup>a</sup>

Key Laboratory of Eco-Textiles, Ministry of Education, Jiangnan University, Wuxi 214122, Jiangsu, China

Received 17 June 2015; revised received and accepted 27 July 2015

Polyamide 6 (PA6), polyacrylonitrile (PAN) and cellulose acetate (CA) have been prepared by electrospinning. Electrospun CA nanofibres are deacetylated to obtain cellulose nanofibres. Polyaniline (PANI)-based composite nanofibres have been prepared by *in situ* polymerization of aniline with the electrospun PA6, PAN and cellulose nanofibres separately. Structural and chemical examinations of the prepared composite nanofibres are conducted by scanning electron microscope and Fourier transform infrared spectroscopy. The sensing properties of the PANI-based composite nanofibres to ammonia are evaluated by a home-made sensor test system. It is found that PA6/PANI, PAN/PANI and cellulose/PANI composite nanofibres respond to ammonia. Cellulose/PANI composite nanofibres show the best ammonia sensing properties among them, whose response to 250 ppm ammonia is found to be 2.70, followed by PA6/PANI (1.52) and PAN/PANI's (1.23).

**Keywords:** Ammonia sensing, Cellulose, Polyacrylonitrile, Polyamide 6, Polyaniline composite

## 1 Introduction

Due to its distinctive redox property, controllable conductivity and good thermal stability<sup>1,2</sup>, PANI has attracted a great deal of attention for application in sensors<sup>3</sup>, batteries<sup>4</sup>, electrochromic materials<sup>5</sup>, electromagnetic shielding materials<sup>6,7</sup>, metal anticorrosion<sup>8</sup> and tissue engineering<sup>9</sup>. In addition, compared with other conductive polymers, such as polypyrrole and polyacetylene, the preparation method of PANI is relatively simple and low cost. However, PANI is infusible, insoluble, almost non-processable<sup>10</sup>, and its physical and mechanical properties are not satisfactory for some applications. These shortcomings hinder its potential applications in various areas.

Many studies dedicating for improving the practical applications of PANI have been explored and reported. Blending PANI with other polymers to fabricate a film or fibres<sup>11-14</sup> is one of the most common techniques. Picciani *et al.*<sup>13</sup> produced nonwoven mats prepared with the mixture of poly (lactic acid) (PLA) and PANI. Peng *et al.*<sup>14</sup> employed electrospun conductive polyaniline-poly(lactic acid) (PAN-PLA) composite nanofibres as counter electrodes for designing rigid and flexible dye-sensitized solar cells. The average diameter of the nanofibres was found about 200 nm. However, in this

method, the conductivity of the composite materials is found inferior to pure PANI as a result of the insulations of most common polymers. Some researchers<sup>15, 16</sup> have tried direct spinning of PANI since it can be dissolved in some solvents, e.g. N-methyl-2-pyrrolidone, chloroform, concentrated sulfuric acid, etc. Pure PANI fibres and blended PANI fibres could be produced by wet-spinning<sup>17-21</sup>. Zhang *et al.*<sup>18</sup> prepared PANI fibres using wet-spinning process and different coagulation solvents or solutions. The resulting fibres exhibited good length, stability, and morphology. Kajekar *et al.*<sup>19</sup> synthesized PANI-nanofibres by interfacial polymerization technique. The prepared PANI-nanofibres were dispersed in n-methyl-2-pyrrolidone (NMP) solvent and then blended with polyvinylpyrrolidone (PVP)/ polysulfone (PSf) for preparing the novel hollow fibre membrane by dry wet spinning technique. The pure water flux, percentage rejection, antifouling property and thermal resistance increased with an increase in PANI-nanofibre concentration. However, the high conjugated structure and strong intermolecular interaction in the molecules of PANI cause hard processability, so the mechanical and electrical properties of PANI need further improvement<sup>17</sup>. Some other researchers<sup>17, 22</sup> have investigated the coating methods of aniline on fibre substrate. The post-treatment is easy to operate and economical<sup>17</sup>. Xin *et al.*<sup>17</sup> dispersed emeraldine base polyaniline (PANI-EB) in the formic acid aqueous solution and

<sup>a</sup>Corresponding author.  
E-mail: qfwei@jiangnan.edu.cn

stirred. Then the dispersed PANI was coated on PA6 fibre by using a coating machine. However, the fastness of the coating was very low, which could affect the potential used of this technique.

Electrospinning is capable of producing nanofibres<sup>23</sup>. Electrospun nanofibres possess many extraordinary properties, such as small diameters, large specific surface areas, etc<sup>24</sup>. For gas sensor, specific surface area is one of the most important properties. With larger surface area, much more functional materials can be exposed to gases. PANI can be fabricated by *in situ* polymerization of aniline using the electrospun fibrous membrane as a template<sup>25, 26</sup>. PANI-based composite nanofibres prepared by this method can possess good conductivity, good fibre structure and large specific surface areas.

In this work, PA6, PAN and cellulose acetate nanofibres were prepared by electrospinning, and polyaniline-based composite nanofibres was produced by *in situ* polymerization of aniline with electrospun PA6, electrospun PAN and regenerated cellulose as templates. The ammonia sensing properties of the PANI-based composite nanofibres were studied and discussed.

## 2 Materials and Methods

### 2.1 Materials

PA6 ( $M_w = 2.1 \times 10^4$  g/mol) was obtained from Zig Zheng Industrial Co. Ltd of Taiwan. PAN ( $M_w = 5.0 \times 10^4 \sim 6.0 \times 10^4$  g/mol) was purchased from American Integrity Group Ltd. Cellulose acetate (CA, 39.8 wt% of acetyl content,  $M_n = 30,000$ ), sodium hydroxide (NaOH), absolute ethyl alcohol, aniline (An), ammonium persulfate (APS), ammonia and hydrochloric acid (HCl, concentration 37 %), formic acid (FA), N, N-dimethylformamide (DMF), acetone and N,N-dimethylacetamide (DMAc) were purchased from Sinopharm Chemical Reagent Co. Ltd. (Beijing, China). All chemicals and reagents were used as received, except for aniline, which was distilled twice before use. Distilled water was used in this study.

### 2.2 Preparation of Nanofibres

Nanofibres were prepared by electrospinning. The parameters of precursor solutions and electrospinning

are given in Table 1. Electrospinning was carried out using a syringe with a spinneret diameter of 0.5 mm. The positive electrode of the high-voltage power supply was attached to the metal needle tip while the grounded stainless drum was used as the collector wrapped with aluminum foil and rotated at 20 rpm. The thickness of the fibrous mats was about 10  $\mu\text{m}$  controlled by the spinning time.

Because of their hydrophobicity, the electrospun CA nanofibres were deacetylated in 0.05 M NaOH in ethanol for 12 h to regenerate cellulose nanofibres. After that the obtained cellulose nanofibres were washed with distilled water for three times to remove residual NaOH and ethanol.

### 2.3 Preparation of PANI Composite Nanofibres

The *in situ* polymerization of aniline was carried out in an ice/water bath at 0-5 °C. The as-prepared nanofibre membranes were first immersed in 230 mL of 1.2 M HCl solution containing a certain amount of aniline. Aniline molecules in the solution were adsorbed on the surface of the nanofibres with the help of interaction force between them. About 30 min later, 20 mL of 1 M HCl solution containing APS was slowly added into the above solution to initiate the polymerization. The mole ratio of aniline to APS was 1:1. Successive polymerization was lasted for 5 h. At last, the samples were taken out and washed with deionized water, and dried in vacuum at 50 °C for 24 h.

### 2.4 Characterizations

The morphologies of all nanofibres were examined by a field emission scanning electron microscope (FESEM, S-4800, Hitachi, Tokyo, Japan). Fourier transform infrared (FTIR) spectra were obtained in the range of 4000-400  $\text{cm}^{-1}$  with a 4  $\text{cm}^{-1}$  spectral resolution by using a NEXUS 470 spectrometer (Nicolet, Madison, WI, USA). The wetting behavior of nanofibres was evaluated by contact angles. The contact angles of the nanofibres were measured by dataphysics device. (DCAT 21, Dataphysics instruments GmbH, Tübingen, Germany).

### 2.5 Ammonia Sensing Test

The samples were pasted onto sensing electrode and the sensing behavior for  $\text{NH}_3$  was investigated

Table 1 — Precursor solutions and spinning parameters<sup>27-29</sup>

Polymer	Solvent	Solute percentage	Voltage kV	Feeding rate mL/h	Receive distance cm
PA6	Formic acid	20	20	0.3	20
PAN	N,N-dimethylformamide	10	18	0.5	15
CA	Acetone: N,N-dimethylacetamide (3:2 v/v)	15	18	0.8	16

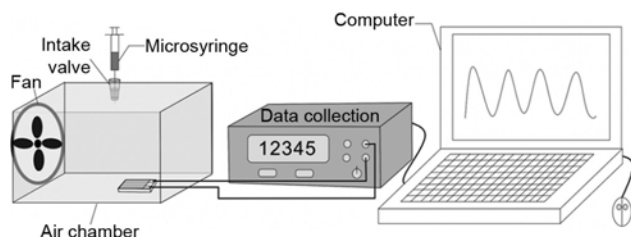


Fig. 1 — Schematic illustration of home-made gas sensing system with a home-made test system (Fig. 1). The tests were conducted at room temperature ( $25 \pm 1^\circ\text{C}$ ) with a relative humidity of  $65 \pm 1\%$ . During the tests, the actual ammonia volume injected into the air chamber was 0.6734, 1.3468, 2.0202 and 2.693  $\mu\text{L}$  corresponding to the ammonia vapor concentration of 50, 100, 150 and 200 ppm respectively. After the ammonia was injected into the air chamber, the resistance of the sensors was recorded for 400 s, and then the test chamber was flushed with dry air consecutively for another 800 s to make sure that a relatively steady state has been achieved before the next cyclic test. The definition of gas response is the ratio of  $(R_i - R_0)/R_0$ , wherein  $R_i$  and  $R_0$  are the resistance of sensors in testing gas and in air respectively<sup>24</sup>. Each result reported was the average of five tests.

### 3 Results and Discussion

#### 3.1 Surface Morphology and Contact Angles

The surface morphologies of the prepared nanofibres were observed by SEM. The surface wetting behaviors were investigated by static contact angle measurements.

As shown in Fig. 2, the electrospun CA, regenerated cellulose, PA6 and PAN nanofibres show smooth surface and fibre network structure. Their water contact angles are also presented in Fig. 2. It is observed that the contact angles of PA6 and PAN are  $44.6^\circ$  and  $41.7^\circ$  respectively. It is also found that the contact angle changes from  $133.6^\circ$  to  $16.5^\circ$ , when CA nanofibres are deacetylated to cellulose nanofibres. The contact angle of cellulose is much smaller than those of PA6 and PAN, and during the contact angle test, the dropped water is adsorbed by cellulose very quickly (completely adsorbed in 1 s), while the water droplet could be hold for a while on the surface of PA6 and PAN nanofibres. The change in surface hydrophilicity would facilitate the adsorption of aniline molecules from the solution onto the nanofibre surface.

The SEM images of pure PA6, PAN, cellulose fibres and their corresponding PANI composite

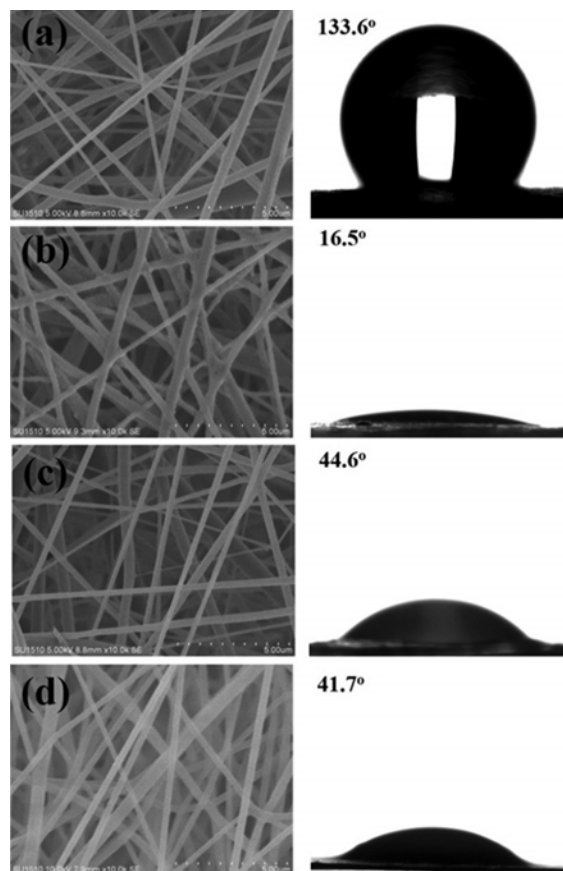


Fig. 2 — SEM images of (a) CA, (b) cellulose, (c) PA6, and (d) PAN nanofibres and their corresponding water contact angles

nanofibres are shown in Fig. 3. It can be clearly observed that the surfaces of PANI composite nanofibres become rough as compared to the original nanofibres, because of the existence of PANI. The SEM images clearly reveal that a thin layer of PANI grows on the surfaces of PA6, PAN and cellulose fibres after *in situ* polymerization of aniline. However, the PANI composite nanofibres still maintain the fibrous network structure after the surface deposition of PANI. With fibrous structure, the PANI-based composite nanofibres could provide a large surface area which improves the gas sensing properties of these nanofibres.

#### 3.2 FTIR Analysis

The FTIR spectra of pure nanofibres and their PANI composite nanofibres are shown in Figs 4 (a) – (c). In Fig. 4 (a), the C=O stretching vibration peak of amide in PA6 is found at  $1637.22\text{ cm}^{-1}$ , while the C=O stretching vibration peak of PA6/PANI is observed at  $1634.37\text{ cm}^{-1}$ . The peak shifts may be caused by hydrogen bond and Van der Waals force between PANI and PA6. In Fig. 4(b), the peak at

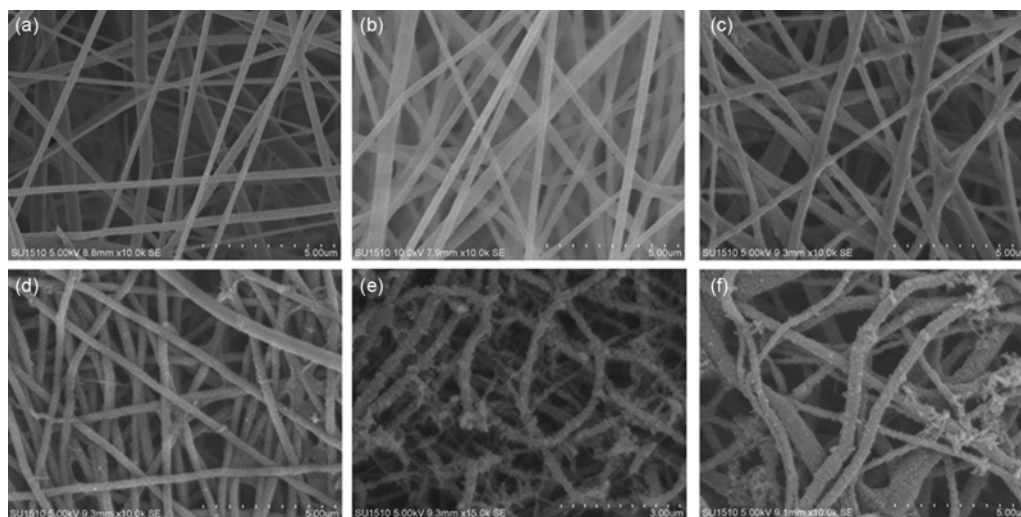


Fig. 3 — SEM images of (a) PA6, (b) PAN, (c) cellulose nanofibres, (d) PA6/PANI, (e) PAN/PANI and (f) cellulose/PANI composite nanofibres

around  $2242.79\text{ cm}^{-1}$  is assigned to  $\text{C}\equiv\text{N}$  stretching vibrations of the PAN molecular chain for the PAN nanofibres. For PAN/PANI, the peak at  $2240.60\text{ cm}^{-1}$  corresponds to  $\text{C}\equiv\text{N}$  of PAN in PAN/PANI nanofibres. The characteristic peak of  $\text{C}=\text{C}$  stretching vibrations of benzene is found at around  $1485.11\text{ cm}^{-1}$ , and the characteristic peak of  $\text{C}-\text{N}$  stretching vibration of the secondary aromatic amine is found at around  $1301.97\text{ cm}^{-1}$ . These two peaks are identical to PANI. The FTIR spectra of cellulose nanofibres [ Fig. 4 (c)] exhibits the adsorption bands at  $3347.14\text{ cm}^{-1}$  and  $2890.85\text{ cm}^{-1}$ , assigned to the stretching vibration of  $\text{O}-\text{H}$  and the asymmetrically stretching vibration of  $\text{C}-\text{H}$  respectively. Compared with the spectrum of cellulose nanofibres, it is found that the peak at  $3347.14\text{ cm}^{-1}$  and  $2890.85\text{ cm}^{-1}$  are shifted to about  $3243.03\text{ cm}^{-1}$  and  $2917.62\text{ cm}^{-1}$  respectively. The shifts of the spectra indicate the existence of interaction between PANI and pure nanofibres.

### 3.3 Ammonia Sensing Properties

To investigate the ammonia sensing properties of PANI composite nanofibres, ammonia sensing tests have been performed and ammonia sensing properties of PA6/PANI, PAN/PANI and cellulose/PANI composites nanofibres are compared. The gas concentrations used were 50, 100, 150, 200 and 250 ppm respectively. The changes in resistance of the prepared composite nanofibres with respect to time on the exposure to  $\text{NH}_3$  in one test are shown in Fig. 5 (a). It is obvious that the resistance of the prepared composite nanofibres increases dramatically when

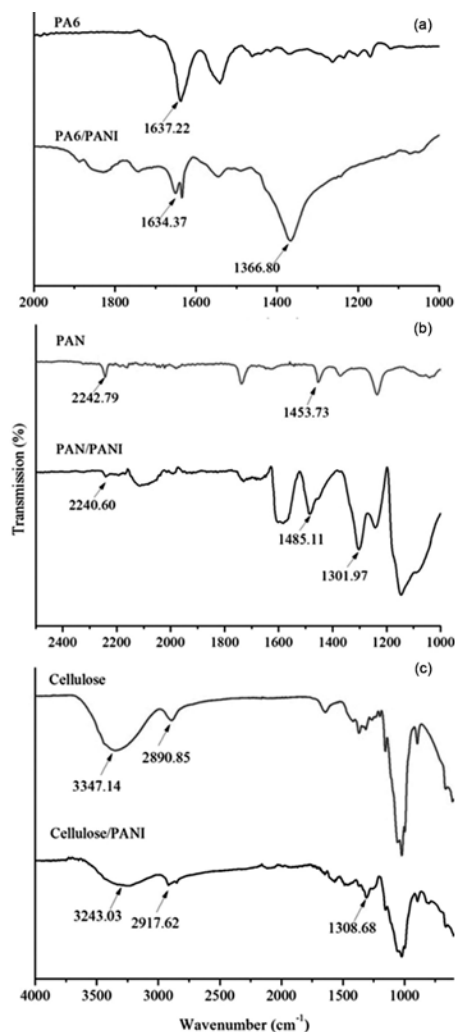


Fig. 4 — FTIR spectra of pure and composite nanofibres: (a) PA6 and PA6/PANI, (b) PAN and PAN/PANI and (c) cellulose and cellulose/PANI nanofibres

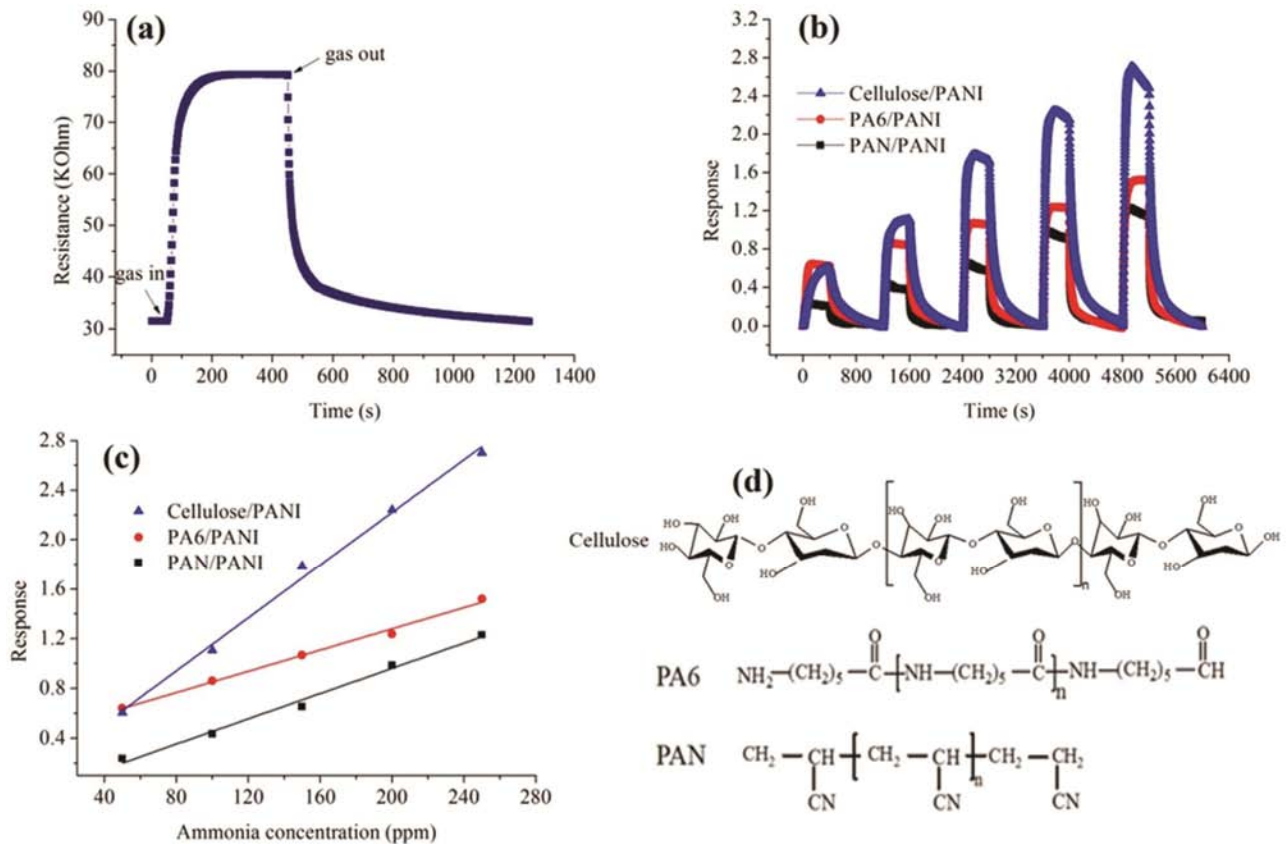


Fig. 5 — (a) Changes in resistance of prepared composite nanofibres with respect to time, (b) dynamic response and recovery of PA6/PANI and PAN/PANI to 50-200 ppm  $\text{NH}_3$ , (c) calibration curves of response values of cellulose/PANI, PA6/PANI and PAN/PANI to 50 -250 ppm  $\text{NH}_3$ , and (d) structures of cellulose, PA6 and PAN

they are exposed to  $\text{NH}_3$ , and later the resistance becomes stable. When the gas room is opened, fresh air is introduced in and the gas blows out, and as a result the resistance is decreased and then returned to the original value gradually.

The dynamic response and recovery of PA6/PANI, PAN/PANI and cellulose/PANI composites nanofibres are shown in Fig. 5 (b). It can be seen that the change trend of the dynamic response of the prepared composite nanofibres is similar to that of their resistance. It is obvious that the response value of cellulose/PANI composite nanofibres is much higher than those of the other two composite nanofibres. For example, when the ammonia concentration is 250 ppm, the response value of cellulose/PANI composite nanofibres is 2.7, but the response value of PA6/PANI is 1.5, while that of PAN/PANI is only 1.23.

Figure 5 (c) shows the response values of the prepared composite nanofibres to 50 - 250 ppm ammonia vapor and their calibration curves. It is obvious that the response values of cellulose/PANI

composite nanofibres were much higher than the others. In particular, the slope of response for the cellulose/PANI composite nanofibres was the highest one. And the slope of response for PA6/PANI was similar to that of PAN/PANI composite nanofibres, but their slopes were much lower compared to cellulose/PANI composite nanofibres. This means that the sensitivity of the cellulose/PANI composite nanofibres was the highest one. The thickness of PA6, PAN and cellulose nanofibres was similar to each other, but their ammonia gas sensing properties were quite different. This may be because that their surface properties were different. As shown in Figure 5 (d), cellulose has many O-H on the surface and PA6 has N-H and C=O, while PAN has  $\text{C}\equiv\text{N}$  which can form hydrogen bonds with aniline. The quantity of O-H of cellulose was much more than that of N-H and C=O of PA6 and  $\text{C}\equiv\text{N}$  of PAN. This may lead to different amount of aniline adsorbed on the surfaces of the electrospun nanofibres. As a result, the quantities of PANI can be exposed to ammonia was the largest for cellulose/PANI composite nanofibres.

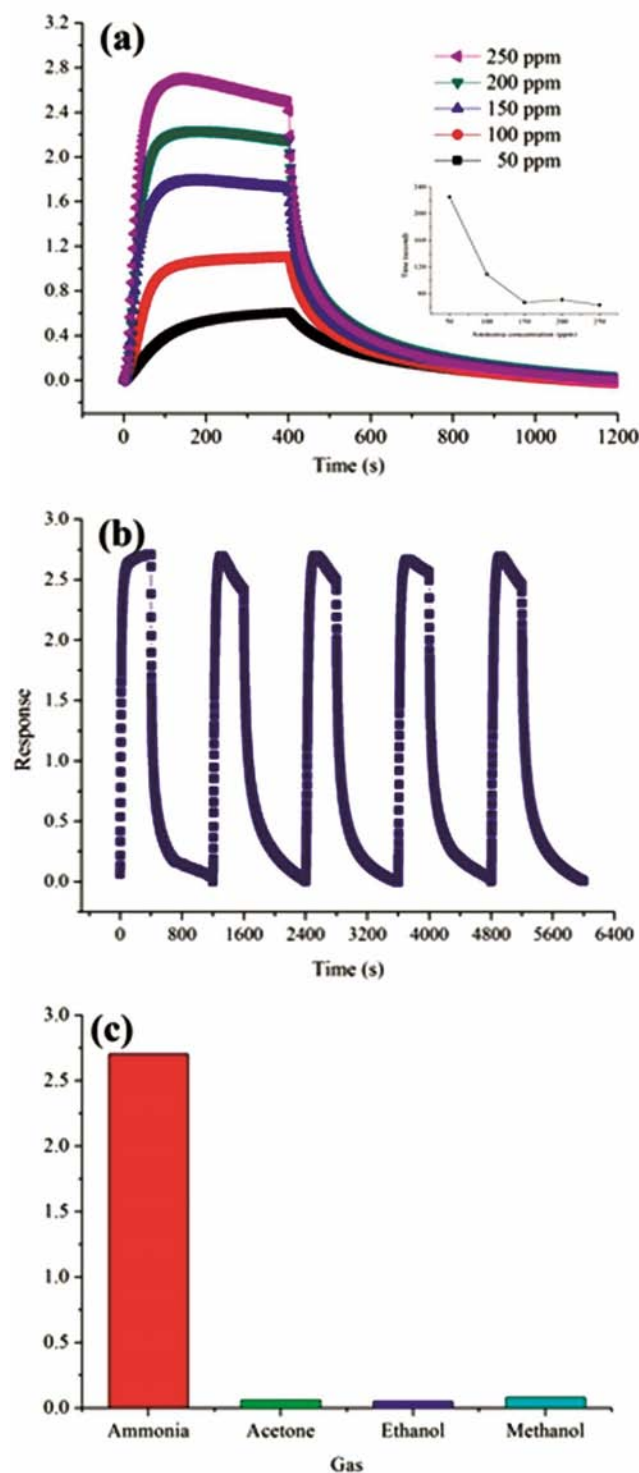


Fig. 6 — (a) Response values of cellulose/PANI composite nanofibres to 50-250 ppm NH<sub>3</sub> and their response time, (b) repeatability of cellulose/PANI composite nanofibres, and (c) response values of cellulose/PANI composite nanofibres to 250 ppm of different gases

As the response values of cellulose/PANI composite nanofibres are the highest among the three composite nanofibre sensors, we also studied its repeatability and selectivity. Figure 6 (a) shows the response values of cellulose/PANI composite nanofibres to 50-250 ppm ammonia and their response time. With the increase in ammonia concentration, the response time of cellulose/PANI composite nanofibres is decreased.

Dynamic response and recovery of cellulose/PANI composite nanofibres gas sensor has been monitored for repeated exposure and removal of 250 ppm ammonia vapor up to five cycles. It can be observed that they have reliable repeatability [Fig. 6 (b)]. To study their cross sensitivity, the cellulose/PANI composite nanofibres are exposed to 250 ppm acetone, ethanol and methanol respectively. As shown in Fig. 6 (c), there is a distinct difference in their response values to NH<sub>3</sub> and the other gases. The sensors show very weak responses to acetone, ethanol and methanol. In conclusion, the prepared cellulose/PANI composite nanofibre sensor exhibits high selectivity to ammonia.

#### 4 Conclusion

PA6/PANI, PAN/PANI and cellulose/PANI composite nanofibres have been successfully fabricated via combination of electrospinning and *in-situ* polymerization. The surface properties of the electrospun nanofibres play a key role in the formation of composite nanofibres, which would affect the quantity of aniline adsorbed on the surface of the fibres. The ammonia sensing properties of the prepared composite nanofibres indicates that all PA6/PANI, PAN/PANI and cellulose/PANI composite nanofibres have high sensitivity for ammonia detection. The prepared cellulose/PANI composite nanofibres are found the best sensor among them, and their repeatability and cross sensitivity are also reliable.

#### Acknowledgement

Authors acknowledge with thanks the financial support by Changjiang Scholars and Innovative Research Team in University (No.IRT1135), the National Natural Science Foundation of China (No.51163014), the Priority Academic Program Development of Jiangsu Higher Education Institutions, Industry-Academia-Research Joint Innovation Fund of Jiangsu Province (BY2012068),

the Science and Technology Support Program of Jiangsu Province (SBE201201094), and the Innovation Program for Graduate Education in Jiangsu Province (No. CXLX13\_742).

## References

- 1 Olad A & Rashidzadeh A, *Fiber Polym*, 13 (2012) 16.
- 2 Ali S, Genaro A G & Uttandaraman S, *Can J Chem Eng*, 92 (2014) 1207.
- 3 Duong N H, Nguyen T T, Nguyen D T & Le H T, *Sensors-Basel*, 11 (2011) 1924.
- 4 Ma Z L & Kan J Q, *Synthetic Met*, 174 (2013) 58.
- 5 Kang J H, Oh Y J, Paek S M, Hwang S J & Choy J H, *Sol Energ Mat Sol C*, 93 (2009) 2040.
- 6 Marins J A, Soares B G, Fraga M, Muller D & Barra G M O, *Cellulose*, 21 (2014) 1409.
- 7 Tang J Y & Di J F, *J Text Res*, 32 (2011) 148.
- 8 Sathiyarayanan S, Azim S S & Venkatachari G, *Electrochim ACTA*, 52 (2007) 2068.
- 9 Li M Y, Guo Y, Wei Y, MacDiarmid A G & Lelkes P I, *Biomaterials*, 27 (2006) 2705.
- 10 Pan W, Yang S L, Li G & Jiang J M, *Eur Polym J*, 41 (2005) 2127.
- 11 Schettini A R A, Peres R C D & Soares B G, *Synthetic Met*, 159 (2009) 1491.
- 12 da Silva A B & Bretas R E S, *Synthetic Met*, 162 (2012) 1537.
- 13 Picciani P H S, Medeiros E S, Pan Z L, Wood D F, Orts W J, Mattoso L H C & Soares B G, *Macromol Mater Eng*, 295 (2010) 618.
- 14 Peng S J, Zhu P N, Wu Y Z, Mhaisalkara S G & Ramakrishna S, *RSC Adv*, 2 (2012) 652.
- 15 Zhao Y Y, Zhang Z M, Yu L M & Tang Q W, *Synthetic Met*, 212 (2016) 84.
- 16 Srinivasan S S, Ratnadurai R, Niemann M U, Phani A R, Goswami D Y & Stefanakos E K, *Int J Hydrogen Energ*, 35 (2010) 225.
- 17 Jin X, Xiao C F & Wang W Y, *Synthetic Met*, 160 (2010) 368.
- 18 Zhang F, Halverson P A, Lunt B & Linford M R, *Synthetic Met*, 156 (2006) 932.
- 19 Kajekar A J, Dodamani B M, Isloor A M, Karim Z A, Cheer N B, Ismail A F & Shilton S J, *Desalination*, 365 (2015) 117.
- 20 Mirmohseni A, Dorraji M S S & Hosseini M G, *Electrochim ACTA*, 70 (2012) 182.
- 21 Lee S J, Oh H J, Lee H A & Ryu K S, *Synthetic Met*, 135 (2003) 399.
- 22 Yu D X, Cheng J & Yang Z R, *J Mater Sci Technol*, 23 (2007) 529.
- 23 Li X Q, Su Y, Zhou X & Mo X M, *Colloid Surface B*, 69 (2009) 221.
- 24 Li X Q, Lin L, Zhu Y N, Liu W W, Yu T S & Ge M Q, *Polym Composite*, 34 (2013) 282.
- 25 Miao Y E, Fan W, Chen D & Liu T X, *ACS Appl Mater Inter*, 5 (2013) 4423.
- 26 Zhang X, Zhang F H, Li S & Wu X Y, *J Bio Eng Res*, 28 (2009) 39.
- 27 Pang Z Y, Fu J P, Luo L, Huang F L & Wei Q F, *Colloid Surface A*, 461 (2014) 113.
- 28 Zhang P, Zhang J N, Wang Q Q & Wei Q F, *Polym Bull*, 7 (2013) 56.
- 29 Fu J P, Pang Z Y, Yang J, Huang F L, Cai Y B & Wei Q F, *Appl Surf Sci*, 349 (2015) 35.